第38卷第9期 中国科学技术大学学报 Vol. 38, No. 9
2008年9月 JOURNAL OF UNIVERSITY OF SCIENCE AND TECHNOLOGY OF CHINA Sep. 2008

Article ID: 0253-2778(2008)09-1042-09

Numerical study on generalized KdV equations and Ito-type coupled KdV equations

LI Pei-ling, LIU Ru-xun

(*Department of Mathematics, University of Science and Technology of China, Hefei* 230026, *China*)

Abstract: An implicit compact difference Padé scheme was improved to solve the fully nonlinear Korteweg-de Vries (KdV) equations and Ito-type coupled KdV equations. Particularly, this method was applied to study the behaviors of solutions of compacton and Ito-type coupled KdV equations. Numerical results show the effectiveness of this scheme.

Key words: compacton solutions; implicit Padé scheme; fully nonlinear Korteweg-de Vries equations; Ito-type coupled KdV equations

CLC number: O241.82 **Document code**: A

AMS Subject Classification (2000): 65M06

广义 KdV 方程和 Ito 型耦合 KdV 方程的数值研究

李佩玲,刘儒勋

(中国科学技术大学数学系,安徽合肥 230026)

摘要:采用隐式紧差分 Padé 方法解完全非线性 KdV 方程和 Ito 型耦合 KdV 方程.特别地,应用这种方法研究了 compacton 和 Ito 型耦合 KdV 方程的解特性.数值结果证明了这种方法的效果.

关键词:compacton 解;隐式 Padé 方法;完全非线性 KdV 方程;Ito 型耦合 KdV 方程

0 Introduction

In recent years, exact compacton solutions to a large number of nonlinear partial differential equations have been found. It is the realization that such equations possess special solutions in the form of pulses which retain their shapes and velocities after interaction between themselves. The existence of such stable solutions is due to a balance between dispersion and nonlinearity in the partial differential equations. For more details about compacton solutions, consult Refs. [1~4].

An example of a compacton-producing equation is the $K(i,j,p)$ equation[2]:

$$\left.\begin{aligned} u_t+\beta_1(u^i)_x+\beta_2(u^j)_{3x}+\beta_3(u^p)_{5x}=0,\\ i,j,p>1. \end{aligned}\right\} \quad (1)$$

In particular from the exact solutions of Eq. (1) for $\beta_3\neq 0$, the range of the nonlinearity parameters i, j, and p for which compacton solutions are allowed is $2\leqslant i=j=p\leqslant 5$ whereas for $\beta_3=0$ the

Received: 2006-05-15; **Revised**: 2006-09-25

Foundation item: Supported by NNSF of China (90411009).

Biography: LI Pei-ling, female, born in 1981, master. Research field: large-scale scientific computing. E-mail: peiling@ustc.edu

Corresponding author: LIU Ru-xun, Prof. E-mail: liurx@ustc.edu.cn

corresponding range is $2\leqslant i=j=p\leqslant 3$.

We will first show for $\beta_3\neq 0$, the exact solution of (1) is[2]

$$u(x,t)=\begin{cases}A_n\cos^{\delta_n}(B_n(x-\lambda t)),\\ \qquad |\ B_n(x-\lambda t)\ |\leqslant \pi/2;\\ 0,\text{otherwise};\end{cases}\quad (2)$$

where δ_n, A_n and B_n are constants for $n=2,3$ and 5 respectively. For the $K(3,3,3)$ equation,

$$\left.\begin{aligned}\delta_3=2, A_3=2\sqrt{\frac{2\lambda}{5\beta_1}},\\ B_3=\frac{1}{12}\sqrt{\frac{13\beta_1}{\beta_2}}, \beta_3=\frac{36{\beta_2}^2}{169\beta_1};\end{aligned}\right\}\quad (3)$$

and for the $K(5,5,5)$ equation,

$$\left.\begin{aligned}\delta_5=1, A_5=\sqrt[4]{\frac{15\lambda}{8\beta_1}},\\ B_5=\frac{1}{15}\sqrt{\frac{34\beta_1}{\beta_2}}, \beta_3=\frac{225{\beta_2}^2}{1\ 156\beta_1}.\end{aligned}\right\}\quad (4)$$

The fifth-order fully nonlinear $K(i,j,p)$ equations (1) and useful for describing the dynamics of various physical systems.

Another class of partial differential equations that has soliton solutions with compact support is the $Q(i,j,l)$ equation[4], which admits a linear subclass of travelling solutions:

$$u_t+a(u^{i+1})_x+\omega[u(u^j)_{xx}]_x+\delta[u(u^l)_{xxxx}]_x=0.\quad (5)$$

In spite of the differences between the quintic dispersion terms in Eqs. (1) and (5), the emerging patterns are quite similar. Unless otherwise we shall assume that $a=\omega=1$. To find traveling waves with a constant speed we define $s=x-\lambda t$ and integrate once to obtain

$$-\lambda u+u^{i+1}+u(u^j)_s+\delta u(u^l)_{4s}=C_0(=\text{const.})\quad (6)$$

Disregarding the integration constant we cast Eq. (6) into the obvious product $uL[u(s)]$. In particular, if $i=j=l$, we obtain a linear equation in $L[V(s)]$ where $V=u^l$, and

$$L[V(s)]\doteq-\lambda+V+V_{ss}+\delta V_{4s}=0.\quad (7)$$

Eq. (6) has one particular class of compacton solutions which depend on special values of δ, for $\delta=0.16$,

$$V(s)=\begin{cases}\frac{8}{3}\lambda\cos^4(\sqrt{\Delta_-}s/2), |\ \sqrt{\Delta_-}s\ |\leqslant\pi;\\ 0,\text{otherwise};\end{cases}\quad (8)$$

for $\delta=0.09$,

$$V(s)=\begin{cases}2\lambda[2-\cos(\sqrt{\Delta_-}s)]\cos^4(\sqrt{\Delta_-}s/2),\\ \qquad |\ \sqrt{\Delta_-}s\ |\leqslant\pi;\\ 0,\text{otherwise};\end{cases}\quad (9)$$

where $\Delta_-=(1-\sqrt{1-4\delta})/2\delta$. Finite difference and finite element methods have been developed to study $K(n,n)$ equations by Ismail and Taha[5]. In this Paper we develop an implicit compact difference Padé scheme to solve the generalized Korteweg-de Vries (KdV) equations.

Besides, coupled nonlinear equations in which a KdV structure is embedded occur naturally in shallow water wave problems[15]. We will use a numerical method which is similar with the methods dealing with $K(n,n,n)$ equations to study Ito-type coupled KdV equations.

1　Implicit Padé schemes

We will use the following notations for our difference methods: The approximate numerical value of u at the grid point $(x,t)=(mh,nk)$ is denoted by $u_m^n(m=0,1,\cdots,M,\ n=0,1,\cdots,N)$. u^n denotes the numerical value at $n\Delta t$, while u_m denotes the numerical value at $m\Delta x$. Here we set $h=\Delta x$ and $k=\Delta t$.

The first, second, third, forth and fifth space derivatives ($f_x=f'$, $f_{xx}=f''$, $f_{xxx}=f'''$, $f_{xxxx}=f''''$, $f_{xxxxx}=f''''$) may be replaced by the functional values using the compact expression[6,7]:

$$\alpha f'_{m-1}+f'_m+\alpha f'_{m+1}=c_1\frac{f_{m+3}-f_{m-3}}{6h}+b_1\frac{f_{m+2}-f_{m-2}}{4h}+a_1\frac{f_{m+1}-f_{m-1}}{2h},\quad (10)$$

$$\alpha f''_{m-1}+f''_m+\alpha f''_{m+1}=c_2\frac{f_{m+3}-2f_m+f_{m-3}}{9h^2}+b_2\frac{f_{m+2}-2f_m+f_{m-2}}{4h^2}+a_2\frac{f_{m+1}-2f_m+f_{m-1}}{h^2},\quad (11)$$

$$\alpha f'''_{m-1}+f'''_m+\alpha f'''_{m+1}=$$

$$b_3\frac{f_{m+3}-3f_{m+1}+3f_{m-1}-f_{m-3}}{8h^3}+$$

$$a_3\frac{f_{m+2}-2f_{m+1}+2f_{m-1}-f_{m-2}}{2h^3}, \tag{12}$$

$$\alpha f'''_{m-1}+f'''_m+\alpha f'''_{m+1}=$$

$$b_4\frac{f_{m+3}-9f_{m+1}+16f_m-9f_{m-1}+f_{m-3}}{6h^4}+$$

$$a_4\frac{f_{m+2}-4f_{m+1}+6f_m-4f_{m-1}+f_{m-2}}{h^4}, \tag{13}$$

$$\alpha f''''_{m-1}+f''''_m+\alpha f''''_{m+1}=$$

$$b_5\frac{f_{m+4}-10f_{m+2}+16f_{m+1}-16f_{m-1}+10f_{m-2}-f_{m-4}}{12h^5}+$$

$$a_5\frac{f_{m+3}-4f_{m+2}+5f_{m+1}-5f_{m-1}+4f_{m-2}-f_{m-3}}{2h^5}. \tag{14}$$

According to Talor expansion, to reach a truncation error of order $O(h^4)$ in the approximation (10)～(14), we only need[6]

$$\left.\begin{aligned}
&a_1=\frac{2}{3}(\alpha+2),\ b_1=\frac{1}{3}(4\alpha-1),\ c_1=0;\\
&a_2=\frac{4}{3}(1-\alpha),\ b_2=\frac{1}{3}(-1+10\alpha),\ c_2=0;\\
&a_3=2,\ b_3=2\alpha-1;\\
&a_4=2(1-\alpha),\ b_4=4\alpha-1;\\
&a_5=3,\ b_5=2\alpha-2.
\end{aligned}\right\} \tag{15}$$

If we set

$$E^\alpha u_m^n=u_{m+\alpha}^n,$$

$$\hat{\mu}=\frac{1}{2}(E^{\frac{1}{2}}+E^{-\frac{1}{2}}),$$

$$\hat{\delta}=E^{\frac{1}{2}}-E^{-\frac{1}{2}},$$

$$\bar{\delta}=\frac{1}{2}(E-E^{-1}),$$

$$\bar{\mu}=\frac{1}{2}(E+E^{-1}).$$

$$\hat{\delta}^2=E-2+E^{-1},$$

$$\hat{\mu}\hat{\delta}=\frac{1}{2}(E^{\frac{1}{2}}+E^{-\frac{1}{2}})(E^{\frac{1}{2}}-E^{-\frac{1}{2}})=\frac{1}{2}(E-E^{-1})=\bar{\delta},$$

$$\bar{\mu}\bar{\delta}=\frac{1}{4}(E+E^{-1})(E-E^{-1})=\frac{1}{4}(E^2-E^{-2}).$$

Then Padé simulation of space derivatives ($f_x=f'$, $f_{xx}=f''$, $f_{xxx}=f'''$, $f_{xxxx}=f''''$, $f_{xxxxx}=f'''''$) with a truncation error of $O(h^4)$ can be written as operator form as follows:

$$(1+2\alpha\bar{\mu})f'_m=\frac{1}{h}(b_1\bar{\mu}\bar{\delta}+a_1\bar{\delta})f_m, \tag{16}$$

$$(1+2\alpha\bar{\mu})f''_m=\frac{1}{h^2}(b_2\bar{\delta}^2+a_2\hat{\delta}^2)f_m, \tag{17}$$

$$(1+2\alpha\bar{\mu})f'''_m=\frac{1}{h^3}(b_3\bar{\delta}^3+a_3\bar{\delta}\hat{\delta}^2)f_m, \tag{18}$$

$$(1+2\alpha\bar{\mu})f''''_m=\frac{1}{h^4}\left[b_4\left(\frac{2}{3}\bar{\delta}^2\hat{\delta}^2+\frac{1}{3}\hat{\delta}^4\right)+a_4\hat{\delta}^4\right]f_m, \tag{19}$$

$$(1+2\alpha\bar{\mu})f'''''_m=\frac{1}{h^5}\left[b_5\left(\frac{2}{3}\bar{\delta}^3\hat{\delta}^2+\frac{1}{3}\bar{\delta}\hat{\delta}^4\right)+a_5\bar{\delta}\hat{\delta}^4\right]f_m. \tag{20}$$

In this section we only consider the case $i=j=p=3$ in Eq. (1), therefore, we assume $\beta_1=\beta_2=1$, $\beta_3=36/169$ in order to simplify computation, so we get

$$u_t+(u^i)_x+(u^j)_{xxx}+\beta_3(u^p)_{xxxxx}=0. \tag{21}$$

Let $\dot{u}=u_t$ and $f=u^i$, $g=u^j$, $h=u^p$. In order to simplify computation, we set $b_3=0$ in Eq. (15) then we get $\alpha=1/2$. Using Eqs. (10), (12) and (14), then at the $(n+1/2)$th time level, Eq. (21) becomes

$$\frac{1}{2}\dot{u}_{m-1}+\dot{u}_m+\frac{1}{2}\dot{u}_{m+1}+$$

$$P_1(f_{m+2}+10f_{m+1}-10f_{m-1}-f_{m-2})+$$

$$P_3(g_{m+2}-2g_{m+1}+2g_{m-1}-g_{m-2})+$$

$$P_5(-h_{m+4}+18h_{m+3}-62h_{m+2}+74h_{m+1}-74h_{m-1}+62h_{m-2}-18h_{m-3}+h_{m-4})=0, \tag{22}$$

where $P_1=1/12h$, $P_3=1/h^3$, $P_5=\beta_3/12h^5$. This scheme has a truncation error of order $O(h^4)$.

We use a two time levels $(n, n+1)$ scheme, taking

$$\dot{u}_m^{n+1/2}=\frac{1}{k}(u_m^{n+1}-u_m^n)+O(k^2) \tag{23}$$

and employing the midpoint rule[8] to improve the accuracy and stability. Here,

$$u_m^{n+1/2}=\frac{1}{2}(u_m^{n+1}+u_m^n), \tag{24}$$

$$\left.\begin{aligned}
f^{n+1/2}&=(u^{n+1/2})^i,\\
g^{n+1/2}&=(u^{n+1/2})^j,\\
h^{n+1/2}&=(u^{n+1/2})^p.
\end{aligned}\right\} \tag{25}$$

The advantage of using the midpoint rule

rather than an explicit method, is that the midpoint rule does not have the rigid time step restriction $\Delta t=O(h^5)$. Of course, we pay for this by having to solve a system of nonlinear equations, but this can be done by Newton's method [5] which is very fast in convergence.

To study the stability of the scheme (22), the von Neumann method [9] is applied to the linearized version of this equation. The $K(3,3,3)$ equation is linearized by freezing the terms which give nonlinearity. When $i=j=p=3$, Eq. (21) can be written as[10]

$$u_t+3u^2\frac{\partial u}{\partial x}+\frac{\partial^2}{\partial x^2}\left(3u^2\frac{\partial u}{\partial x}\right)+\beta_3\frac{\partial^4}{\partial x^4}\left(3u^2\frac{\partial u}{\partial x}\right)=0. \tag{26}$$

Now by assuming $\sigma=3\bar{u}^2$, where $\bar{u}$ is considered to represent locally the maximum value of u, the resulting linear equation is

$$u_t+\sigma\frac{\partial u}{\partial x}+\sigma\frac{\partial^3 u}{\partial x^3}+\beta_3\sigma\frac{\partial^5 u}{\partial x^5}=0. \tag{27}$$

Since this scheme (22)～(25) is a system of two level schemes, it can be expressed as the following linearized version,

$$\begin{aligned}&\frac{1}{2}(u_{m-1}^{n+1}-u_{m-1}^n)+(u_m^{n+1}-u_m^n)+\frac{1}{2}(u_{m+1}^{n+1}-u_{m+1}^n)+\\&\frac{k}{24h}\sigma[(u_{m+2}^{n+1}+10u_{m+1}^{n+1}-10u_{m-1}^{n+1}-u_{m-2}^{n+1})+(u_{m+2}^n+10u_{m+1}^n-10u_{m-1}^n-u_{m-2}^n)]+\\&\frac{k}{2h^3}\sigma[(u_{m+2}^{n+1}-2u_{m+1}^{n+1}+2u_{m-1}^{n+1}-u_{m-2}^{n+1})+(u_{m+2}^n-2u_{m+1}^n+2u_{m-1}^n-u_{m-2}^n)]+\\&\frac{k}{24h^5}\cdot\beta_3\cdot\sigma[(-u_{m+4}^{n+1}+18u_{m+3}^{n+1}-62u_{m+2}^{n+1}+74u_{m+1}^{n+1}-74u_{m-1}^{n+1}+62u_{m-2}^{n+1}-18u_{m-3}^{n+1}+u_{m-4}^{n+1})+\\&(-u_{m+4}^n+18u_{m+3}^n-62u_{m+2}^n+74u_{m+1}^n-74u_{m-1}^n+62u_{m-2}^n-18u_{m-3}^n+u_{m-4}^n)]=0.\end{aligned} \tag{28}$$

Substitute $u_m^n=e^{\alpha nk}e^{i\beta mh}=\xi^n e^{i\beta mh}$ where $\xi=e^{\alpha k}$, and after some manipulations the amplification factor is given by

$$e^{\alpha k}=\frac{A-iB}{A+iB}, \tag{29}$$

where

$$A=\cos\theta+1,$$

$$\begin{aligned}B=&\left[\frac{k}{12h}\sigma(\sin 2\theta+10\sin\theta)+\right.\\&\frac{k}{h^3}\sigma(\sin 2\theta-2\sin\theta)+\frac{k}{12h^5}\sigma\beta_3(-\sin 4\theta+\\&\left.18\sin 3\theta-62\sin 2\theta+74\sin\theta)\right],\end{aligned}$$

$$\theta=\beta h.$$

From Eq. (29) we can deduce that

$$|e^{\alpha k}|=1 \tag{30}$$

for all θ.

So this scheme is unconditionally stable in the linearized sense. However, for the nonlinear version, we have noticed that this scheme blows up after certain time steps. Even if we reduce the time step size, this can delay the blow up but it will not prevent it. So in order to overcome this difficulty, an artificial dissipation term $\varepsilon\delta_x^6u_m^{n+1}$ is added to Eq. (22).

Now by the addition of the dissipation term to Eq. (28), the amplification factor of Eq. (29) alters and satisfies the following condition:

$$|e^{\alpha k}|^2=\frac{A^2+B^2}{(A+C)^2+B^2}<1, \tag{31}$$

where $C=4\varepsilon\frac{k}{3h^6}(\cos\theta-1)^3>0$ if we choose $\varepsilon<0$.

The choice of ε is a delicate matter which we can choose as small as possible in order not to lose the accuracy and the properties of the differential equations.

2　Modified implicit Padé schemes

For $a=\omega=1$ cases, Eq. (5) can be written as

$$\begin{aligned}&u_t+(u^{i+1})_x+u_x(u^j)_{xx}+u(u^j)_{xxx}+\\&\delta u_x(u^l)_{xxxx}+\delta u(u^l)_{xxxxx}=0.\end{aligned} \tag{32}$$

Set $\alpha=0$ in Eq. (10), the first space derivative ($u_x=u'$) becomes

$$u'_m=\frac{-u_{m+2}+8u_{m+1}-8u_{m-1}+u_{m-2}}{12h}+O(h^4). \tag{33}$$

So the semi-discretization of Eq. (32) in space can

be expressed as below at the point of $i\Delta x$,

$$u_t+(u^{i+1})_x+v_m(u^j)_{xx}+u_m(u^j)_{xxx}+\delta v_m(u^l)_{xxxx}+\delta u_m(u^l)_{xxxxx}+O(h^4)[(u^j)_{xx}+(u^l)_{xxxx}]=0, \tag{34}$$

where

$$v_m=(-u_{m+2}+8u_{m+1}-8u_{m-1}+u_{m-2})/(12h).$$

Let $f=u^{i+1}$, $g=u^j$, $h=u^l$. In order to simplify computation we set $b_4=0$ in (13) then we get $\alpha=1/4$ in Eq. (15), thus at the $(n+1/2)$th time level, Eq. (34) becomes

$$\frac{1}{4}\dot{u}_{m-1}+\dot{u}_m+\frac{1}{4}\dot{u}_{m+1}+P_1\left(\frac{f_{m+1}-f_{m-1}}{2h}\right)+P_2\left(\frac{1}{2}\cdot\frac{f_{m+2}-2f_m+f_{m-2}}{4h^2}+\frac{f_{m+1}-2f_m+f_{m-1}}{h^2}\right)+$$
$$P_3\left(-\frac{1}{2}\cdot\frac{g_{m+3}-3g_{m+1}+3g_{m-1}-g_{m-3}}{8h^3}+2\cdot\frac{g_{m+2}-2g_{m+1}+2g_{m-1}-g_{m-2}}{2h^3}\right)+$$
$$P_4\left(\frac{h_{m+2}-4h_{m+1}+6h_m-4h_{m-1}+h_{m-2}}{h^4}\right)+P_5\left(3\,\frac{h_{m+3}-4h_{m+2}+5h_{m+1}-5h_{m-1}+4h_{m-2}-h_{m-3}}{2h^5}-\right.$$
$$\left.\frac{1}{2}\cdot\frac{h_{m+4}-10h_{m+2}+16h_{m+1}-16h_{m-1}+10h_{m-2}-h_{m-4}}{12h^5}\right)=0, \tag{35}$$

where

$$P_1=3/2, P_2=v_m,$$
$$P_3=u_m, P_4=3/2\delta v_m, P_5=\delta u_m.$$

The scheme has a truncation of order

$$O(k^2+h^4+u_x h^4+(u^j)_{xx}h^4+(u^l)_{xxxx}h^4).$$

Due to the lack of smoothness at the edge of a compacton, u_x is not continuous at the edge of curves, therefore, the value of $(u^j)_{xx}$ is unpredictable or infinite at the same point. According to error estimation above, the oscillation at the edge of solution curves appears, which will be shown in Example 3.2. However, by continued mesh refinement, the numerical solutions of the $Q(i,j,l)$ equation (5) will become less oscillatory at the tail of curves.

The stability analysis is similar to the $K(3,3,3)$ equation.

3 Numerical examples and results

To illustrate the efficiency of the proposed numerical method in studying the nonlinear dynamics of solutions of the model equations (1) and (5), some test examples are solved in the following.

Example 3.1 In this example we first show the accuracy test result of $K(3,3,3)$ and $K(5,5,5)$ equations in Tab. 1. We also show the single compacton propagation in Fig. 1 for the initial condition

$$u(x,0)=\begin{cases}A\cos^{\delta}(B(x-x_0)),\\ \qquad |B(x-x_0)|\leqslant\pi/2;\\ 0,\ \text{otherwise};\end{cases} \tag{36}$$

where δ, A and B are defined in Eq. (3) for $K(3,3,3)$, assuming $\beta_1=\beta_2=1$.

Example 3.2 In this example we first show the accuracy test result of $Q(2,2,2)$ equation[4]

$$u_t+(u^3)_x+(u(u^2)_{xx})_x+\delta(u(u^2)_{xxxx})_x=0 \tag{37}$$

in Tab. 2 with the exact solution: for $\delta=0.16$

$$u(x,t)=\begin{cases}\sqrt{\frac{8}{3}\lambda}\cos^2(\sqrt{\Delta_-}(x-\lambda t)/2),\\ \qquad |\sqrt{\Delta_-}(x-\lambda t)|\leqslant\pi;\\ 0,\ \text{otherwise};\end{cases} \tag{38}$$

and with the exact solution: for $\delta=0.09$,

$$u(x,t)=\begin{cases}\sqrt{2\lambda[2-\cos(\sqrt{\Delta_-}(x-\lambda t))]}\cos^2(\sqrt{\Delta_-}(x-\lambda t)/2),\\ \qquad \sqrt{\Delta_-}(x-\lambda t)|\leqslant\pi;\\ 0,\ \text{otherwise}.\end{cases} \tag{39}$$

Next, we proceed to show the single compacton propagation in Fig. 2 for the initial condition

$$u(x,0)=\begin{cases}\sqrt{\frac{8}{3}\lambda}\cos^2(\sqrt{\Delta_-}(x-x_0)/2),\\ \qquad |\sqrt{\Delta_-}(x-x_0)|\leqslant\pi;\\ 0,\ \text{otherwise}.\end{cases} \tag{40}$$

Tab. 1　Accuracy test for one-compacton experiment of $K(i,j,p)$ equation (1) with the exact solution (2), where $\beta_1=\beta_2=1$. Periodic boundary condition, $x_0=0$. $K(3,3,3)$ and $K(5,5,5)$ equation with N points at $t=10$, $k=0.01$

N	$K(3,3,3)$				$K(5,5,5)$			
	L_1 error	order	L_∞ error	order	L_1 error	order	L_∞ error	order
50	6.08E−03	—	2.44E−02	—	1.40E−02	—	8.54E−02	—
100	4.67E−04	3.70	3.48E−03	2.81	3.33E−03	2.07	4.09E−02	1.06
200	4.06E−05	3.52	7.40E−04	2.23	5.67E−04	2.55	1.06E−02	1.95
400	2.84E−06	3.84	9.51E−05	2.96	1.24E−04	2.19	4.98E−03	1.09

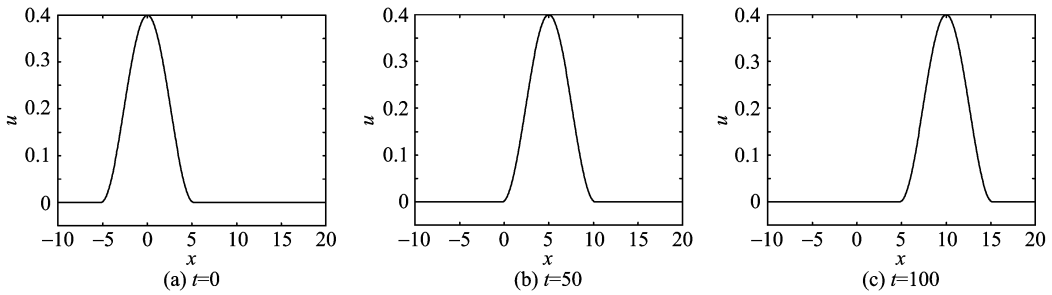

Fig. 1　The single compacton solution of $K(3,3,3)$, $x_0=0$, $\lambda=0.1$. The initial data is taken as Eqs. (3) and (36), using 400 points in $[-10,20]$.

Tab. 2　Accuracy test for one-compacton experiment of the $Q(2,2,2)$ equation (37) with the exact solution (38) and (40). Periodic boundary condition, $x_0=-5$, $\delta=0.16$ and $\delta=0.09$ with N points at $t=10$, $k=0.01$

N	$\delta=0.16$				$\delta=0.09$			
	L_1 error	order	L_∞ error	order	L_1 error	order	L_∞ error	order
375	3.25E−03		2.41E−02	—	4.91E−03	—	3.58E−02	—
750	8.32E−04	1.97	8.93E−03	1.43	1.42E−03	1.79	1.39E−02	1.37
1500	2.67E−04	1.64	3.93E−03	1.18	3.86E−04	1.88	5.66E−03	1.29
3000	9.93E−05	1.43	1.84E−03	1.10	1.27E−04	1.60	2.55E−03	1.15

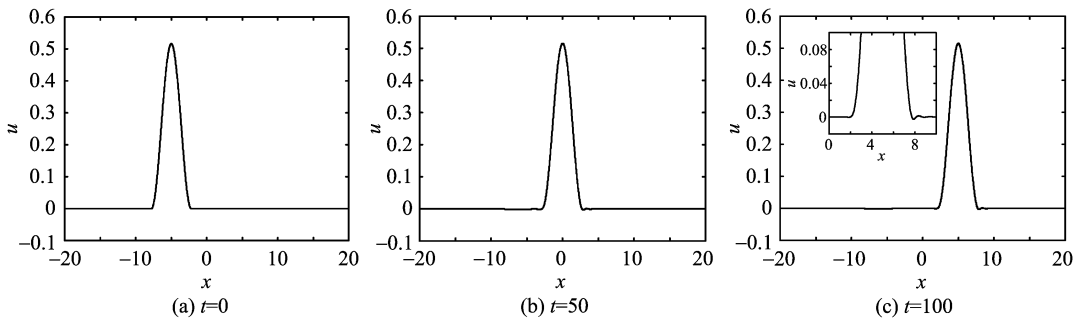

Fig. 2　The single compacton solution of $Q(2,2,2)$, $\delta=0.16$, $x_0=-5$, $\lambda=0.1$. The initial data is taken as Eq. (39), using 2 667 points in $[-20,20]$.

We also show the single compacton propagation in Fig. 3 for the initial condition:

$$u(x,0)=\begin{cases}\sqrt{2\lambda[2-\cos(\sqrt{\Delta_-}(x-x_0))]}\cos^2(\sqrt{\Delta_-}(x-x_0)/2),\\ \qquad |\sqrt{\Delta_-}(x-x_0)|\leqslant\pi;\\ 0,\ \text{otherwise.}\end{cases}\tag{41}$$

Example 3.3　In this example we first show the accuracy test for $K(2,2)$ and $K(3,3)$ equations[1] in Tab. 3.

$K(2,2)$ equation

$$u_t+(u^2)_x+(u^2)_{xxx}=0\tag{42}$$

has the exact solution

$$u_c(x,t)=\begin{cases}\frac{4}{3}v\cos^2(\xi/4),\ |\xi|=|x-vt|\leqslant 2\pi;\\ 0,\ \text{otherwise;}\end{cases}\tag{43}$$

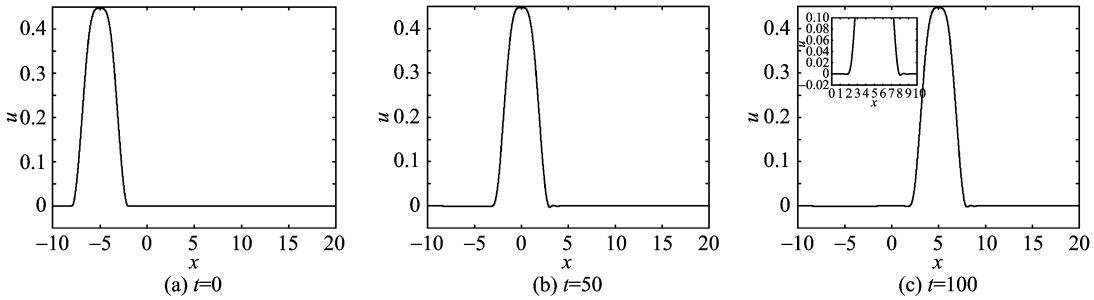

Fig. 3 The single compacton solution of $Q(2,2,2)$, $\delta=0.09$, $x_0=-5$, $\lambda=0.1$. The initial data is taken as Eq. (41), using 3 000 points in $[-10,20]$.

Tab. 3 Accuracy test for one-compacton experiment. Periodic boundary condition, $v=2$, $x_0=0$. $K(2,2)$ and $K(3,3)$ equation with N points in $[-10,50]$ at $t=10$, $k=0.1$

N	$K(2,2)$				$K(3,3)$			
	L_1 error	order	L_∞ error	order	L_1 error	order	L_∞ error	order
50	3.45E−01	—	1.90E−00	—	3.31E−01	—	1.78E−00	—
100	5.85E−02	2.56	3.64E−01	2.38	7.65E−02	2.11	6.12E−01	1.54
200	1.16E−02	2.33	8.43E−02	2.11	6.26E−03	3.61	7.14E−02	3.04
400	2.07E−03	2.49	1.53E−02	2.46	1.32E−03	2.25	1.87E−02	1.94

with below initial condition

$$u(x,0)=\begin{cases}\frac{4}{3}v\cos^2(x/4), & |x|\leqslant 2\pi;\\ 0, & \text{otherwise.}\end{cases} \tag{44}$$

$K(3,3)$ equation

$$u_t+(u^3)_x+(u^3)_{xxx}=0 \tag{45}$$

has the exact solution

$$u_c(x,t)=\begin{cases}\pm\sqrt{3v/2}\cos(\xi/3), & |\xi|=|x-vt|\leqslant 3\pi/2;\\ 0, & \text{otherwise.}\end{cases} \tag{46}$$

We solve Eq. (45) subject to the inital condition

$$u(x,0)=\begin{cases}\sqrt{3v/2}\cos(x/3), & |x|\leqslant 3\pi/2;\\ 0, & \text{otherwise.}\end{cases}$$

For implicit Padé scheme, an artificial dissipation term $\varepsilon\delta_x^4 u_m^{n+1}$ is added to this scheme for $K(n,n)$ equation, where $\varepsilon>0$ according to stability analysis.

Because they all bear compact support, "compactons" interact with each other until the moment of collision. Therefore, the initial conditions are delicately chosen to give three compactons on a collision course.

For the collisions of $K(2,2)$ equations, as Fig. 4, with the following initial condition

$$u(x,0)=\sum_{j=1}^{3}u_{c,j}(x,0) \tag{47}$$

where

$$u_{c,j}=\begin{cases}\frac{4}{3}v_j\cos^2((x-D_j)/4), & |x-D_j|\leqslant 2\pi;\\ 0, & \text{otherwise;}\end{cases} \tag{48}$$

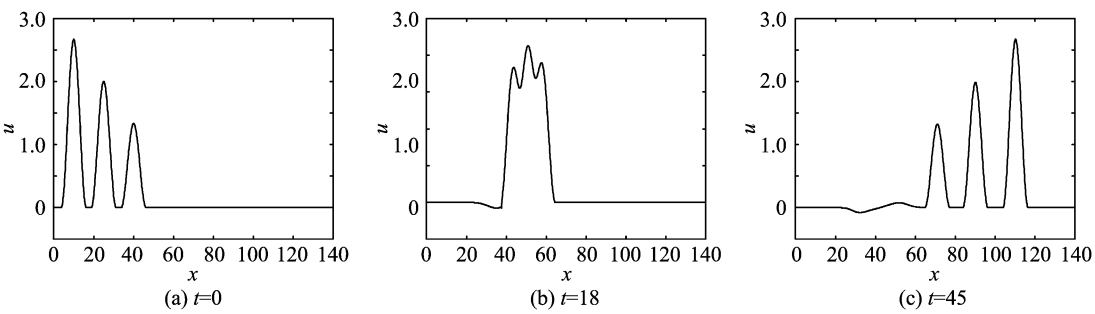

Fig. 4 The evolution of three $K(2,2)$ compactons with speeds $v=2, 1.5$ and 1 starting with centers $x=10, 25$ and 40

$$D_1 = 10, D_2 = 25, D_3 = 40,$$
$$v_1 = 2, v_2 = 1.5, v_3 = 1.0.$$

For the collisions of $K(3,3)$ equations, as Fig. 5, with the following initial condition

$$u(x,0) = \sum_{j=1}^{3} u_{c,j}(x,0), \tag{49}$$

$$u_{c,j}(x,0) = \begin{cases} \sqrt{(3v_j/2)}\cos((x-D_j)/3), & |x-D_j| \leqslant 3\pi/2; \\ 0, & \text{otherwise}; \end{cases} \tag{50}$$

where

$$\left.\begin{aligned} &D_1 = 10, D_2 = 25, D_3 = 40, \\ &v_1 = 2, v_2 = 1.5, v_3 = 1.0. \end{aligned}\right\} \tag{51}$$

From the numerical experiments we have found that the three compactons recover their shapes after the collision (see Fig. 4 and Fig. 5). After the reemergence of compactons in Fig. 4 and Fig. 5, the collision site is marked by the birth of a small-amplitude, zero-mass, compact ripple, which very slowly evolves into compacton-anticompacton pairs. Typically, the maximum amplitudes (and velocities) of newly created compacton-anticompacton pairs are less than 1/20 of the original compacton's amplitude. We can compare these results with Ref. [1]. The lack of smoothness at the edge of the compacton reduces the numerical precision and introduces dispersive errors into the calculation that are difficult to distinguish from radiation created in a nonelastic collision except by continued mesh refinement. A further numerical difficulty is caused by the delicate balance in the nonlinear dispersion. When expanded, it has a diffusion like term $2u_x u_{xx}$. On the trailing edge of the compacton $u_x > 0$ and this term acts like a destabilizing backward diffusion operator.

Example 3.4　Ito-type coupled KdV equations:

$$\left.\begin{aligned} &u_t + \alpha u u_x + \beta v v_x + \gamma u_{xxx} = 0, \\ &v_t + \beta(uv)_x = 0, \end{aligned}\right\} \tag{52}$$

where α, β, and γ are arbitrary constants. For $\alpha = -6, \beta = -2, \gamma = -1, \delta = -2$, Eq. (52) represents the Ito's equation which describes the interaction process of two internal long waves and has infinitely many conserved quantities[11]. It is noted that this choice of parameters is not unique[13]. In Ref. [14], it is shown that this coupled system can be a member of a bi-Hamiltonian integrable hierarchy.

In this example we show the numerical results for the Ito's equation by implicit Padé scheme.

$$\left.\begin{aligned} &u_t - (3u^2 + v^2)_x - u_{xxx} = 0, \\ &v_t - 2(uv)_x = 0, \end{aligned}\right\} \tag{53}$$

with an initial condition

$$\left.\begin{aligned} &u(x,0) = \cos(x), \\ &v(x,0) = \cos(x). \end{aligned}\right\} \tag{54}$$

We also choose a Gaussian initial condition

$$\left.\begin{aligned} &u(x,0) = \exp(-x^2), \\ &v(x,0) = \exp(-x^2). \end{aligned}\right\} \tag{55}$$

From Fig. 6, 7, 8 and 9 we can see that the result for u behaves like dispersive wave solutions and the results for v behaves like shock wave solutions. We can verify these figures with Ref. [16].

4　Conclusion

We have developed a high-order implicit compact difference Padé scheme to solve fully nonlinear Korteweg-de Vries equations and have

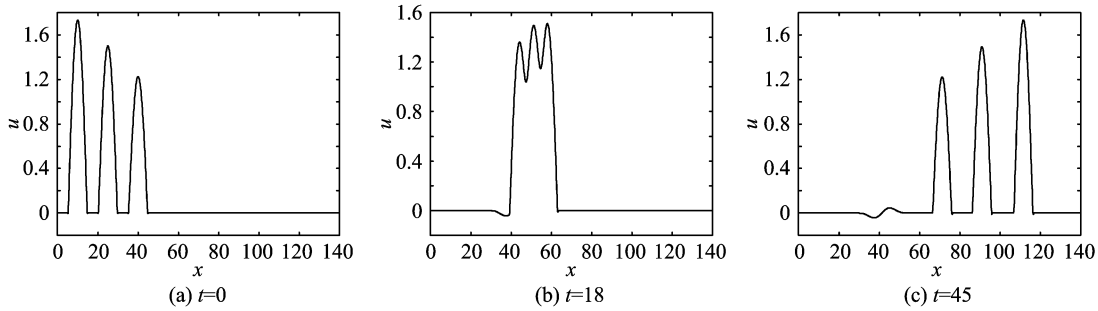

Fig. 5　The evolution of three $K(3,3)$ compactons with speed $v=2, 1.5$ and 1 starting with centers $x=10, 25$ and 40

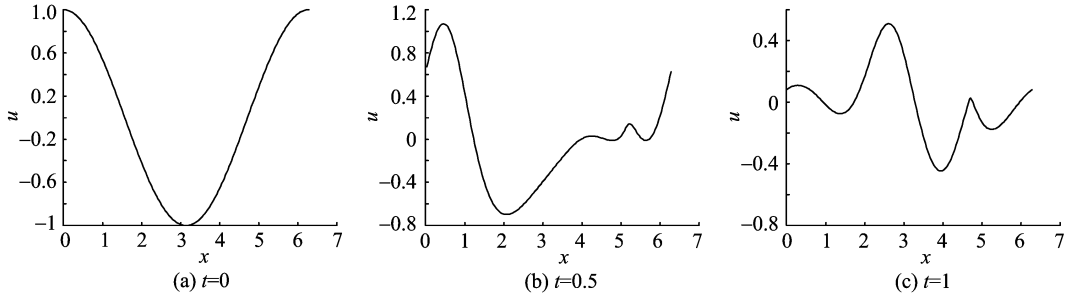

Fig. 6 Numerical results of u for the Ito's equation (53) with the initial condition (54). Periodic boundary condition in $[0, 2\pi]$, using 200 points

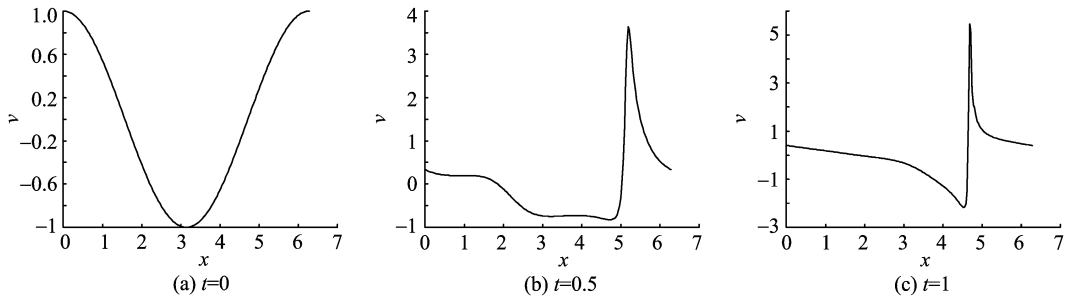

Fig. 7 Numerical results of v for the Ito's equation (53) with the initial condition (54). Periodic boundary condition in $[0, 2\pi]$, using 200 points

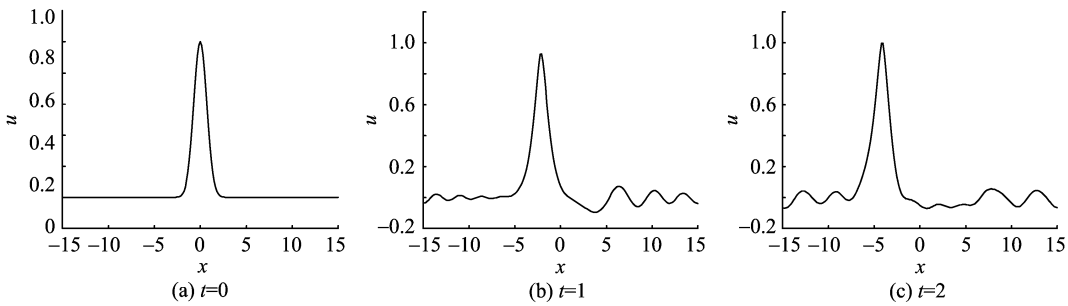

Fig. 8 Numerical results of u for the Ito's equation (53) with the initial condition (55). Periodic boundary condition in $[-15, 15]$, using 200 points

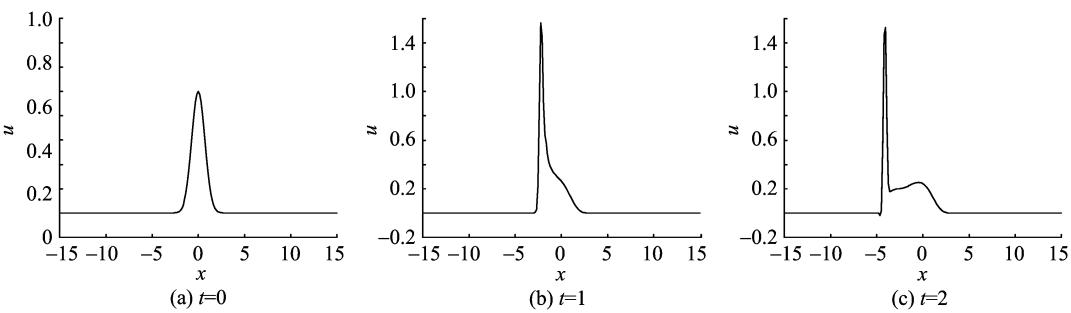

Fig. 9 Numerical results of v for the Ito's equation (53) with the initial condition (55). Periodic boundary condition in $[-15, 15]$, using 200 points

proven its stability and achieved high accuracy numerical results. The schemes we present extend the previous work of Refs. [6, 7] on compact different Padé scheme solving partial differential equations with higher spatial derivatives. The elastic collision between $K(n, n)$ equation is studied by numerical experiments. Numerical examples for Ito-type coupled KdV equations are shown to illustrate the accuracy and capability of this method.

(下转第 1 067 页)

[4] Hu J, Wang X, Zhao K. Verma modules over generalized Virasoro algebras Vir[J]. J Pure Appl Algebra,2003, 177(1): 61-69.
[5] Osborn J M, Zhao K. $\mathbf{Z}\times\mathbf{Z}$-graded Lie algebras containing a Virasoro algebra and a Heisenberg algebra [J]. Comm Algebra, 2001, 29:1 677-1 707.
[6] Shen R, Su Y. Classification of irreducible weight modules with a finite-dimensional weight space over twisted Heisenberg-Virasoro algebra [J]. Acta Mathematica Sinica, English Series, 2007, 23(1): 189-192.
[7] Su Y, Zhao K. Second cohomology group of generalized Cartan type Witt Lie algebras and central extensions[J]. Comm Algebra, 2002, 30: 3 285-3 309.
[8] Wang X. Verma modules over generalized Block algebras B(b(1); b(2)) [J]. Comm Algebra, 2006, 34(2): 415-424.
[9] Wang X, Zhao K. Verma modules over Virasoro-like algebras[J]. J Aust Math Soc, 2006, 80(2):179-191.
[10] Zhu L, Su Y. Non-graded Virasoro and super-Virasoro algebras and modules of intermediate series[J]. Journal of Mathematical Research and Exposition, 2006, 26(2):325-333 (in Chinese).

(上接第 1 050 页)

References

[1] Rosenau P, Hyman J M. Compactons: Solitons with finite wavelengths[J]. Phys. Rev. Lett., 1993, 70(5): 564-567.
[2] Dey B. Compacton solutions for a class of two parameter generalized odd-order Korteweg-de Vries equations[J]. Phys. Rev. E, 1998, 57(4): 4 733-4 738.
[3] Ludu A, Stoitcheva G, Draayer J P. Similarity analysis of nonlinear equations and bases of finite wavelength solitons[J]. Int. J. Modern Physics E: Nuclear Physics, 2000, 9(3): 263-278.
[4] Rosenau P, Levy D. Compactons in a class of nonlinearly quintic equations[J]. Physics Letters A, 1999, 252: 297-306.
[5] Ismail M S, Taha T R. A numerical study of compactons [J]. Mathematics and Computers in Simulation, 1998, 47(6): 519-530.
[6] Lele S K. Compact finite difference schemes with spectral-like resolution[J]. J. Comp. Phys., 1992, 103:16-42.
[7] Liu Ru-xun, Wu Ling-ling. Small-stencil Padé scheme to solve, nonlinear evolution equation[J]. Applied Mathematics and Mechanics, 2005, 26:801-809.
[8] Holden H, Karlsen K H, Risebro N H. Operator splitting methods for generalized Korteweg-de Vries equations[J]. J. Comp. Phys., 1999, 153:203-222.
[9] Mitchell A R, Griffiths D F. The Finite Difference Method in Partial Differential Equations[M]. New York: Wiley, 1980.
[10] Richtmyer R D, Morton K W. Difference Methods for Initial Value Problems [M]. New York: Wiley/Interscience, 1967.
[11] Ito M. Symmetries and conservation laws of a coupled nonlinear wave equation[J]. Physics Letters A, 1982, 91: 335-338.
[12] Rosenau P. On nonanalytic solitary waves formed by a nonlinear dispersion[J]. Phys. Lett. A, 1997, 230: 305-318.
[13] Antonowicz M, Fordy A P. Coupled KdV equations with multi-Hamiltonian structures [J]. Physica D, 1987, 28: 345-357.
[14] Kupershmidt B A. A coupled Korteweg-de Vries equation with dispersion[J]. Journal of Physics A: Mathematical and General, 1985, 18: L571-L573.
[15] Whitham G. Linear and Nonlinear Waves[M]. New York: Wiley, 1974.
[16] Xu Y, Shu C W. Local discontinuous Galerkin methods for the Kuramoto-Sivashinsky equations and the Ito-type coupled KdV equations [J]. Computer Methods in Applied Mechanics and Engineering, 2006, 195: 3 430-3 447.